

Wafer-scale 30° twisted bilayer graphene epitaxially grown on $Cu_{0.75}Ni_{0.25}$ (111)

Peng-Cheng Ma(马鹏程), Ao Zhang(张翱), Hong-Run Zhen(甄洪润), Zhi-Cheng Jiang(江志诚), Yi-Chen Yang(杨逸尘), Jian-Yang Ding(丁建阳), Zheng-Tai Liu(刘正太), Ji-Shan Liu(刘吉山), Da-Wei Shen(沈大伟), Qing-Kai Yu(于庆凯), Feng Liu(刘丰), Xue-Fu Zhang(张学富), and Zhong-Hao Liu(刘中灏),

Citation: Chin. Phys. B, 2024, 33 (**6**): 066101. DOI: 10.1088/1674-1056/ad2d53
Journal homepage: http://cpb.iphy.ac.cn; http://iopscience.iop.org/cpb

What follows is a list of articles you may be interested in

Geometries and electronic structures of Zr_nCu(n =2-12) clusters: A joint machine-learning potential density functional theory investigation

Yizhi Wang(王一志), Xiuhua Cui(崔秀花), Jing Liu(刘静), Qun Jing(井群), Haiming Duan(段海明), and Haibin Cao(曹海宾)
Chin. Phys. B, 2024, 33 (**1**): 016109. DOI: 10.1088/1674-1056/acd5c2

Ultrafast dynamics in photo-excited Mott insulator $Sr_3Ir_2O_7$ at high pressure

Xia Yin(尹霞), Jianbo Zhang(张建波), Wang Dong(王东), Takeshi Nakagawa, Chunsheng Xia(夏春生), Caoshun Zhang(张曹顺), Weicheng Guo(郭伟程), Jun Chang(昌峻), and Yang Ding(丁阳)
Chin. Phys. B, 2024, 33 (**1**): 016103. DOI: 10.1088/1674-1056/acdc8c

Applications and potentials of machine learning in optoelectronic materials research: An overview and perspectives

Cheng-Zhou Zhang(张城洲) and Xiao-Qian Fu(付小倩)
Chin. Phys. B, 2023, 32 (**12**): 126103. DOI: 10.1088/1674-1056/ad01a4

Pressure-induced phase transition and electronic structure evolution in layered semimetal $HfTe_2$

Mei-Guang Zhang(张美光), Lei Chen(陈磊), Long Feng(冯龙), Huan-Huan Tuo(拓换换), Yun Zhang(张云), Qun Wei(魏群), and Pei-Fang Li(李培芳)
Chin. Phys. B, 2023, 32 (**8**): 086101. DOI: 10.1088/1674-1056/acd2bf

Effects of atomic corrugations on electronic structures in $Pb_{1-x}Bi_x$ thin films

Pengju Li(李鹏举), Kun Xie(谢鹍), Yumin Xia(夏玉敏), Desheng Cai(蔡德胜), and Shengyong Qin(秦胜勇)
Chin. Phys. B, 2023, 32 (**6**): 066101. DOI: 10.1088/1674-1056/acbf29

Wafer-scale 30° twisted bilayer graphene epitaxially grown on $Cu_{0.75}Ni_{0.25}$ (111)

Peng-Cheng Ma(马鹏程)[1,2,†], Ao Zhang(张翱)[3,4,†], Hong-Run Zhen(甄洪润)[1,2], Zhi-Cheng Jiang(江志诚)[3,4], Yi-Chen Yang(杨逸尘)[3,4], Jian-Yang Ding(丁建阳)[3,4], Zheng-Tai Liu(刘正太)[3,4], Ji-Shan Liu(刘吉山)[3,4], Da-Wei Shen(沈大伟)[5], Qing-Kai Yu(于庆凯)[3,4], Feng Liu(刘丰)[1,2,‡], Xue-Fu Zhang(张学富)[3,4,§], and Zhong-Hao Liu(刘中灏)[1,2,¶]

[1] *School of Physical Science and Technology, Ningbo University, Ningbo* 315211, *China*
[2] *Institute of High-Pressure Physics, Ningbo University, Ningbo* 315211, *China*
[3] *National Key Laboratory of Materials for Integrated Circuits, Shanghai Institute of Microsystem and Information Technology, Chinese Academy of Sciences, Shanghai* 200050, *China*
[4] *Center of Materials Science and Optoelectronics Engineering, University of Chinese Academy of Sciences, Beijing* 100049, *China*
[5] *National Synchrotron Radiation Laboratory, University of Science and Technology of China, Hefei* 230029, *China*

(Received 28 November 2023; revised manuscript received 3 February 2024; accepted manuscript online 26 February 2024)

Twisted bilayer graphene (TBG) has been extensively studied because of its novel physical properties and potential application in electronic devices. Here we report the synthesis and characterization of 30° TBG naturally grown on $Cu_{0.75}Ni_{0.25}$ (111) film and investigate the electronic structure by angle-resolved photoemission spectroscopy. Compared with other substrates, our TBG with a wafer scale is acquired with a shorter growth time. The Fermi velocity and energy gap of Dirac cones of TBG are comparable with those of a monolayer on $Cu_{0.85}Ni_{0.15}$ (111). The signature of moiré lattices has not been observed in either the low-energy electron diffraction patterns or the Fermi surface map within experimental resolution, possibly due to different Cu and Ni contents in the substrates enhancing the different couplings between the substrate and the first/second layers and hindering the formation of a quasiperiodic structure.

Keywords: twisted bilayer graphene, electronic structure, Cu/Ni (111)

PACS: 61.48.Gh, 68.65.Pq, 71.28.+d, 81.05.ue **DOI:** 10.1088/1674-1056/ad2d53

1. Introduction

Van der Waals coupled two-dimensional (2D) bilayer materials can be twisted between each layer, and the interlayer twist angle provides an exotic degree of freedom for the emergence of various physical phenomena.[1–12] Twisted bilayer graphene (TBG) comprises two stacked and misaligned monolayer sheets. Stacking order has a strong impact on the coupling between the two layers and determines its physical properties. For small twist angles, magic-angle TBG hosts superconductivity, magnetism, insulating states and quantized anomalous Hall states which emerge from correlation electron states by interlayer coupling.[3–8] For large twist angles, there are no correlation electrons in a wide range of twist angles, but with interlayer hybridization of electronic states under chiral crystal symmetry the crossed nonlinear dynamical Hall effect can arise.[9–12] There are reports of 30° TBG being naturally grown on SiC (0001),[9] Pt (111)[10] and Cu (111)[13] by chemical vapor deposition (CVD), and Dirac cones with twelve-fold rotational symmetry were observed by angle-resolved photoemission spectroscopy (ARPES).[9,10] Without translational symmetry, the charge Hall effect can be expected from the twisted interface coupling.[11,12]

Previously, we have successfully grown wafer-scale high-quality wrinkle-free single-crystalline graphene (SCG) epitaxially on $Cu_{0.85}Ni_{0.15}$ (111) film at a relatively low temperature of 750 °C;[14] this is much lower than the temperature threshold of epitaxial graphene on Cu (111) (about 1000 °C). The low growth temperature not only decreases the energy costs but also solves the problems of high contamination, metal evaporation and wrinkles due to the mismatch of thermal expansion coefficients between the substrate and graphene. The electronic structure of SCG on Cu/Ni (111) has also been studied by ARPES,[15] and the gap size of the Dirac cone is smaller than that of SCG on Cu (111), possibly due to less translational symmetry breaking induced by the Cu/Ni (111) substrate.

In this work, we describe epitaxial growth of centimeter-scale steady 30° TBG on $Cu_{0.75}Ni_{0.25}$ (111) film by CVD and characterize it by optical imaging (OM), scanning electron microscopy (SEM), Raman spectroscopy and low-energy electron diffraction (LEED). Compared with growth on other substrates, our TBG is acquired in a shorter growth time of only 20 min and with a wafer-scale on Cu/Ni (111). Fur-

†These authors contributed equally to this work.
‡Corresponding author. E-mail: liufeng@nbu.edu.cn
§Corresponding author. E-mail: zhangxuefu@mail.sim.ac.cn
¶Corresponding author. E-mail: liuzhonghao@nbu.edu.cn

© 2024 Chinese Physical Society and IOP Publishing Ltd

ther, we investigate the electronic structure of TBG and find Dirac cone-like dispersion comparable to that of a monolayer on Cu/Ni (111) but with the chemical potential shift down to around 164 meV. Our work provides a quick and efficient method to grow large-scale high-quality graphene that could benefit future applications.

2. Experiments

The 30° TBG was synthesized by CVD on $Cu_{0.75}Ni_{0.25}$ (111) thin film at 1050 °C with 500 sccm Ar, 50 sccm H_2 and 50 sccm CH_4 for 60 min for pretreatment at atmospheric pressure. Subsequently, the CH_4 was shut off and the sample was rapidly cooled under the same Ar and H_2 gas flow. The source of Cu/Ni alloy contains 75% Cu and 25% Ni atoms. Various experiments were used to characterize TBG, including Raman spectroscopy, OM and LEED.

ARPES measurements were conducted at the Dreamline and 03U beamlines of the Shanghai Synchrotron Radiation Facility (SSRF). The energy and angular resolutions were set to 15 meV and 0.2°, respectively. The samples were heated from room temperature to 400 °C and then kept at 400 °C for 4 h in the ultra-high vacuum (UHV) chamber to clean the surfaces before measurements. During the measurements, the temperature was kept at 20 K, and the pressure was maintained at better than 6.7×10^{-9} Pa.

3. Results and discussion

Figure 1 shows the manufacturing process of TBG on a $Cu_{0.75}Ni_{0.25}$ (111) substrate by CVD. $Cu_{0.75}Ni_{0.25}$ (111) thin film is fabricated on Al_2O_3 (0001) for graphene epitaxy. The thermodynamics-controlled nucleation process and the kinetics-controlled growth process can precisely tailor the stacking order and morphology of the bilayer graphene. The first nucleation layer of graphene is deposited on $Cu_{0.75}Ni_{0.25}$ (111) with identical orientation because of the regulation of the single-crystal substrate. Then the second layer of graphene domains was formed in the same way but with 30° rotation relative to the first layer; this is a possible metastable state due to the collaborative effect of both Cu/Ni single-crystal and the first layer graphene. Subsequently, the graphene film domains of the two graphene layers seamlessly stitched and formed TBG.

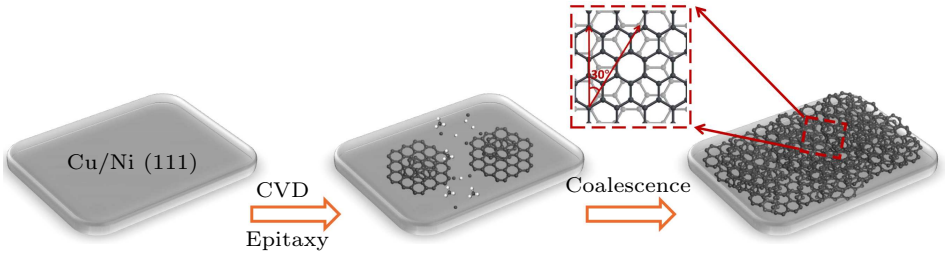


Fig. 1. Schematic diagram of the experimental design for natural growth of 30° TBG on $Cu_{0.75}Ni_{0.25}$ (111).

Figures 2(a)–2(b) show the ultra-flat 30° TBG film grown on $Cu_{0.75}Ni_{0.25}$ (111) characterized by SEM and Raman spectroscopy, respectively. Based on our experience in fabricating graphene on Cu/Ni (111), we have observed that a multilayer is more likely to form under certain conditions with a Ni content of more than about 20%, while a monolayer forms with a Ni content of less than around 20%. Indeed, identifying a monolayer region in large-size TBG on a $Cu_{0.75}Ni_{0.25}$ (111) background poses a challenge. We have made significant efforts to locate a monolayer region in our sample, which exhibits clear differences from the TBG region in the SEM image and the peaks of Raman shifts, as shown in Figs. 2(a) and 2(b). From the SEM image of the Cu/Ni surface coated with graphene (Fig. 2(a)) it is clear that there is a discernible color contrast, which is due to the differences in the number of graphene layers present. To confirm the number of layers, we conducted Raman spectroscopy measurements in the two regions (Fig. 2(b)). These indicate that the G peak and 2D peak heights in region I are almost identical, suggesting that it is double-layer graphene. Conversely, the contrast between the G peak and 2D peak in region II is pronounced, indicating that it is single-layer graphene.

LEED measurements were adapted to investigate the orientation structure and layers for monolayer and TBG grown on Cu/Ni (111) alloy film with different Ni contents. As shown in Fig. 2(c), the LEED pattern of the graphene grown on $Cu_{0.85}Ni_{0.15}$ (111) with 15% Ni shows only one set of diffraction patterns with aligned six-fold rotational symmetric spots arranged in a suitable honeycomb lattice, indicating SCG with uniform size and orientation. As shown in Fig. 2(d), the graphene grown on $Cu_{0.75}Ni_{0.25}$ (111) shows two sets of diffraction patterns with aligned six-fold rotation rotational symmetric spots arranged in a suitable honeycomb lattice, indicating two layers SCG with 30° rotation with respect to each other. The domain structure and the atom arrangement of TBG according to the LEED pattern are shown in Figs. 2(e)–2(f).

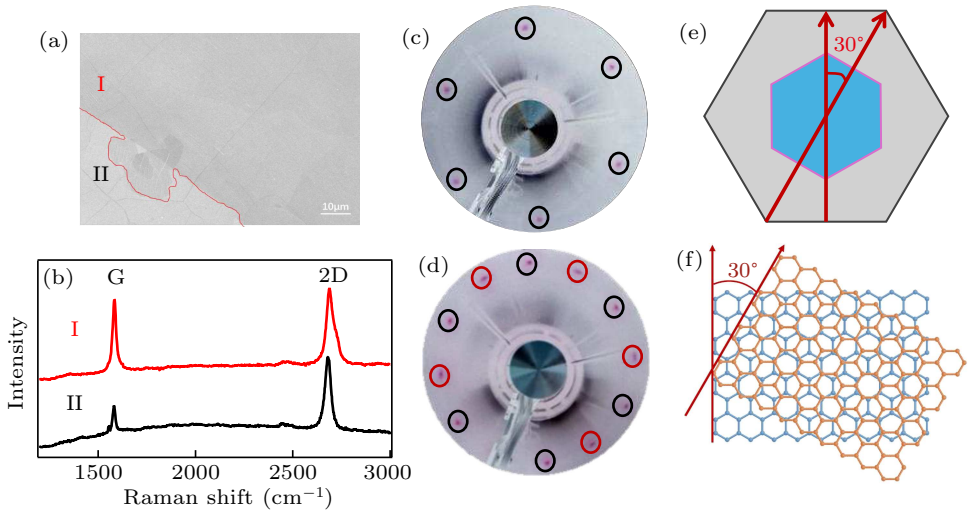


Fig. 2. Characterization of 30° TBG on $Cu_{0.75}Ni_{0.25}$ (111). (a), (b) SEM morphology images and Raman spectra of TBG and monolayer graphene (region I, TBG; region II, monolayer graphene). (c), (d) LEED patterns of monolayer graphene on $Cu_{0.85}Ni_{0.15}$ (111) and TBG on $Cu_{0.75}Ni_{0.25}$ (111). (e) Schematic structure of the graphene domain with the two superimposed concentric hexagons rotated by 30°. (f) An atomic structure model of TBG with 30° rotation.

To study the low-energy electronic structure, we perform numerical calculations for monolayer, bilayer and twisted bilayer graphene at a 30° orientation around the K and K' points utilizing the tight-binding model, as shown in Fig. 3. Owing to graphene's distinctive crystal structure, a Dirac cone manifests at both K and K' points, illustrated in Fig. 3(a) for the K point. Bilayer graphene exhibits two prevalent stacking patterns: AA stacking and AB stacking. In the case of AA stacking, the paired Dirac cones at K and K' do not split but experience a shift by approximately 0.3 eV due to interlayer coupling, as depicted in Fig. 3(b). For AB stacking, one of the paired Dirac cones develops a small gap while the other remains, as shown in Fig. 3(c). TBG at 30° assumes a quasi-crystal structure where the top and bottom layers cannot achieve commensurate periods. To derive the quasi-band structure of TBG at 30°, we employ the 15/26 approximant method,[16] which starts from AA stacking and introduces slight stress to the top layer, altering the lattice constant from 2.456 Å to 2.454 Å. In this approximant, a commensurate period of $15 \times \sqrt{3} \times 2.454 = 26 \times 2.456$ for both the top and bottom layers of graphene is achieved. The unit cell of the 15/26 approximant for tight-binding calculations is illustrated in the inset of Fig. 3(d). Due to the moiré pattern induced by the 30° rotation, the first Brillouin zone of TBG encompasses 12 K and K' points. As illustrated in Fig. 3(d), each K and rotated K point exhibits a Dirac cone originating from the peculiar structure of the twisted bilayer.

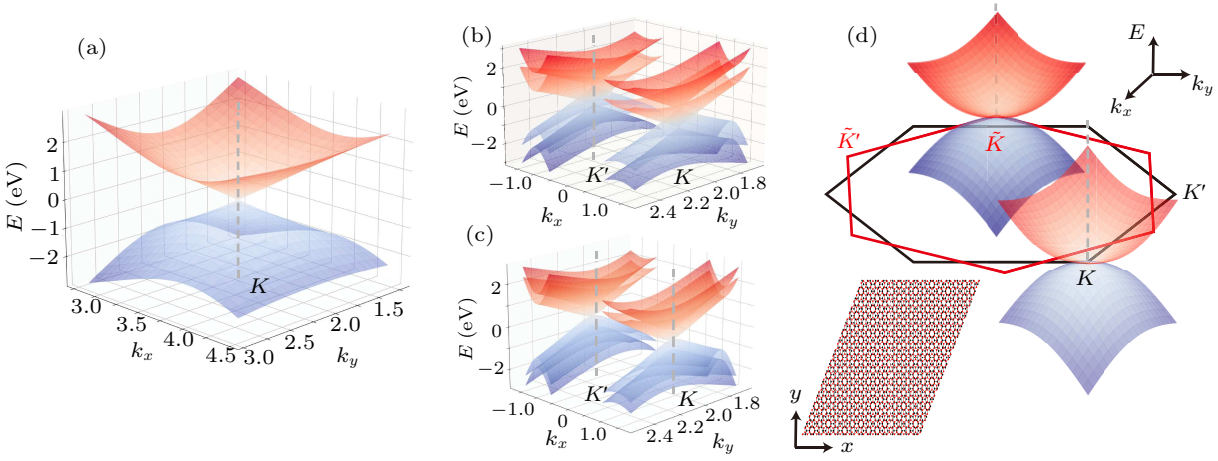


Fig. 3. Numerical calculations of energy band structures of (a) monolayer graphene around the K point, (b), (c) bilayer graphene in AA stacking and AB stacking around K and K' points and (d) 30° TBG around $\tilde{K}$and K. The inset in (d) shows the 15/26 approximant unit cell for simulating the quasi-band structure of 30° TBG.

Subsequently, we experimentally studied the electronic structure of TBG grown on $Cu_{0.75}Ni_{0.25}$ (111) film by ARPES. As shown in Fig. 4, the clear image of the Fermi surface and the Dirac bands indicates the high crystalline quality of the sample. Figure 4(a) shows the integrated intensity plots at the Fermi level (E_F) and −0.6 eV below E_F. As mentioned above, one extra set of bands with 30° rotation is clearly observed relative to the bands of monolayer graphene. The bright spots

at the K_0 and K' points are attributed to the spectra from the two layers. We record the intensity plots at Γ and K' to study the bands, as cut 1 and cut 2 in Fig. 4(b). Figure 4(c) shows the wide valence bands and reveals the s, p and d bands from the Cu/Ni substrate. At the K' point, the crossed linear dispersions form a Dirac cone with a Fermi velocity of approximately 7.3×10^5 m·s^{-1}. For a detailed study of the low-energy dispersions, we show the energy distribution curves and momentum distribution curves centered at the K' point, as shown in Figs. 4(e) and 4(f), respectively. One can see three bands from the energy distribution curves, namely α, β and γ. The α band is the Dirac-like dispersion with a possible energy gap of around 150 meV at the center energy of about 140 meV. The β and γ bands are derived from Cu/Ni sp bands. Compared with monolayer graphene on $Cu_{0.85}Ni_{0.15}$ (111), the chemical potential of TBG shifts down to around 164 meV, possibly due to different interactions and work functions of the metal substrates with different Cu and Ni contents.[17]

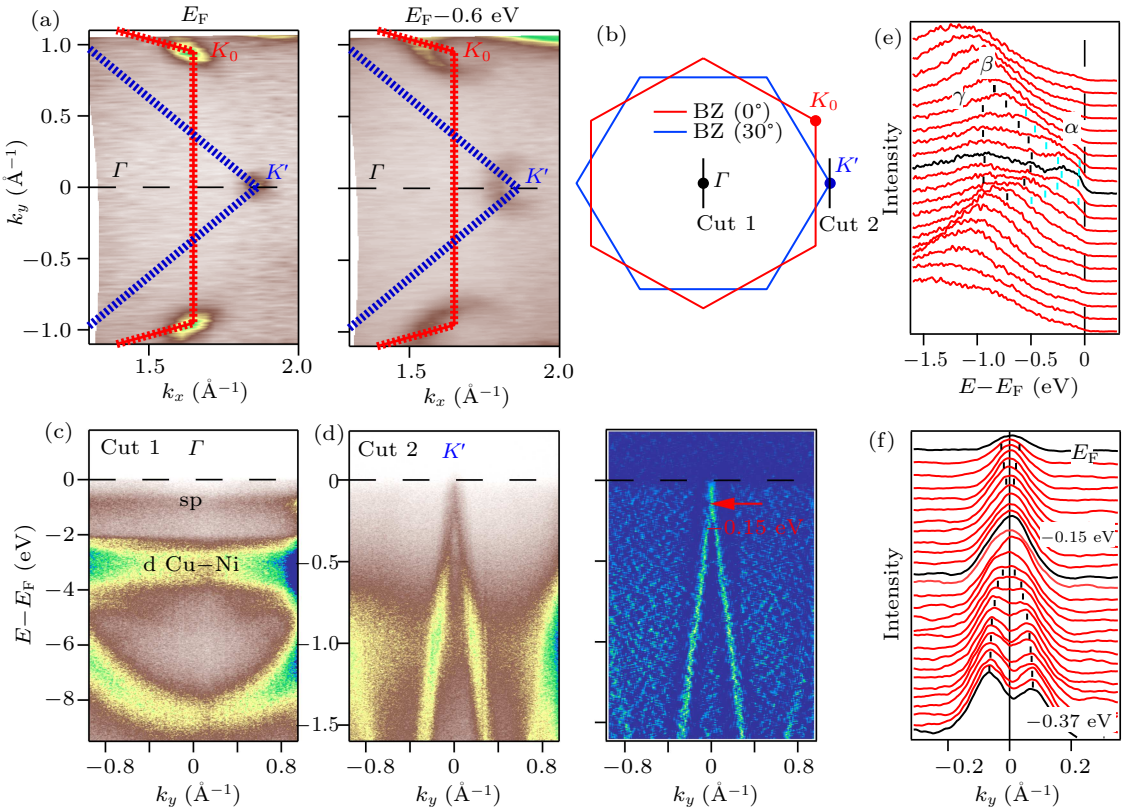


Fig. 4. Femi surface and electronic structure of 30° TBG on $Cu_{0.75}Ni_{0.25}$(111). (a) Integrated photoemission intensity plots (±10 meV) at E_F and −0.6 eV below E_F, respectively. (b) Brillouin zones (BZ) with 0° (red) and 30° (blue) rotations. (c) Photoemission intensity plot along cut 1 as indicated in (b). (d) Photoemission intensity plot and corresponding second derivative plot along cut 2 as indicated in (b). (e), (f) Energy distribution curves and momentum distribution curves around the K' point in (d).

4. Conclusions

In summary, we have reported a new approach for the fabrication of ultra-flat 30° TBG on $Cu_{0.75}Ni_{0.25}$ (111). Compared with growth on the other substrates, our method requires a shorter growth time and achieves wafer-scale high-quality graphene. The electronic structure observed by ARPES reveals two sets of Dirac dispersions with 30° rotation to each other. The Dirac dispersion of TBG is comparable to monolayer graphene on Cu/Ni (111). Our findings suggest that Cu/Ni (111) substrate is a good platform for epitaxial growth of large-scale, high-quality graphene for further study and application of the novel physical properties related to Dirac fermions.

Acknowledgements

Project supported by the National Key R&D Program of China (Grant Nos. 2022YFB3608000 and 2022YFA1204900), the National Natural Science Foundation of China (Grant Nos. 12222413 and 12074205), the Natural Science Foundation of Shanghai (Grant Nos. 23ZR1482200 and 22ZR1473300), the Natural Science Foundation of Zhejiang Province (Grant No. LQ21A040004), and the funding of Ningbo University (Grant No. LJ2024003).

References

[1] Li G, Luican A, Lopes Dos Santos J M B, Castro Neto A H, Reina A, Kong J and Andrei E Y 2010 *Nat. Phys.* **6** 109

[2] Luican A, Li G, Reina A, Kong J, Nair R R, Novoselov K S, Geim A K and Andrei E Y 2011 *Phys. Rev. Lett.* **106** 126802

[3] Wong D, Wang Y, Jung J, Pezzini S, DaSilva A M, Tsai H Z, Jung H S, Khajeh R, Kim Y, Lee J, Kahn S, Tollabimazraehno S, Rasool H, Watanabe K, Taniguchi T, Zettl A, Adam S, MacDonald A H and Crommie M F 2015 *Phys. Rev. B* **92** 155409
[4] Sanchez-Yamagishi J D, Taychatanapat T, Watanabe K, Taniguchi T, Yacoby A and Jarillo-Herrero P 2012 *Phys. Rev. Lett.* **108** 076601
[5] Sanchez-Yamagishi J D, Luo J Y, Young A F, Hunt B M, Watanabe K, Taniguchi T, Ashoori R C and Jarillo-Herrero P 2017 *Nat. Nanotech.* **12** 118
[6] Cao Y, Fatemi V, Fang S, Watanabe K, Taniguchi T, Kaxiras E and Jarillo-Herrero P 2018 *Nature* **556** 43
[7] Cao Y, Fatemi V, Demir A, Fang S, Tomarken S L, Luo J Y, Sanchez-Yamagishi J D, Watanabe K, Taniguchi T, Kaxiras E, Ashoori R C and Jarillo-Herrero P 2018 *Nature* **556** 80
[8] Huang M, Wu Z, Zhang X, Feng X, Zhou Z, Wang S, Chen Y, Cheng C, Sun K, Meng Z Y and Wang N 2023 *Phys. Rev. Lett.* **131** 066301
[9] Ahn S J, Moon P, Kim T H, Kim H W, Shin H C, Kim E H, Cha H W, Kahng S J, Kim P, Koshino M, Son Y W, Yang C W and Ahn J R 2018 *Science* **361** 782
[10] Yao W, Wang E, Bao C, Zhang Y, Zhang K, Bao K, Chan C K, Chen C, Avila J, Asensio M C, Zhu J and Zhou S 2018 *Proc. Natl. Acad. Sci. USA* **115** 6928
[11] Zhai D, Chen C, Xiao C and Yao W 2023 *Nat. Commun.* **14** 1961
[12] Chen C, Zhai D, Xiao C and Yao W 2023 arXiv:2303.09973
[13] Yan Z, Liu Y, Ju L, Peng Z, Lin J, Wang G, Zhou H, Xiang C, Samuel E L G, Kittrell C, Artyukhov V I, Wang F, Yakobson B I and Tour J M 2014 *Angew. Chem. Int. Ed.* **53** 1565
[14] Zhang X, Wu T, Jiang Q, Wang H, Zhu H, Chen Z, Jiang R, Niu T, Li Z, Zhang Y, Qiu Z, Yu G, Li A, Qiao S, Wang H, Yu Q and Xie X 2019 *Small* **15** 1805395
[15] Zhang X F, Liu Z H, Liu W L, Lu X L, Li Z J, Yu Q K, Shen D W and Xie X M 2019 *Chin. Phys. B* **28** 086103
[16] Yu G, Wu Z, Zhan Z, Katsnelson M I and Yuan S 2019 *npj Comput. Mater.* **5** 122
[17] Khomyakov P A, Giovannetti G, Rusu P C, Brocks G, Van Den Brink J and Kelly P J 2009 *Phys. Rev. B* **79** 195425